

NASA TECHNICAL NOTE



NASA TN D-4107

c.1

LOAN COPY
APR
KIRTLAND



NASA TN D-4107

METHODS FOR OBTAINING SURFACE TEMPERATURES OF MATERIALS IN THE PRESENCE OF EXTRANEEOUS RADIATION

by B. L. Schilling
Langley Research Center
Langley Station, Hampton, Va.



**METHODS FOR OBTAINING SURFACE TEMPERATURES OF MATERIALS
IN THE PRESENCE OF EXTRANEEOUS RADIATION**

By B. L. Schilling

**Langley Research Center
Langley Station, Hampton, Va.**

NATIONAL AERONAUTICS AND SPACE ADMINISTRATION

**For sale by the Clearinghouse for Federal Scientific and Technical Information
Springfield, Virginia 22151 - CFSTI price \$3.00**

METHODS FOR OBTAINING SURFACE TEMPERATURES OF MATERIALS IN THE PRESENCE OF EXTRANEOUS RADIATION

By B. L. Schilling
Langley Research Center

SUMMARY

The problem of measuring surface brightness temperatures of materials surrounded by hot radiating gases is discussed. Effects of extraneous radiation on the accuracy of measurements made by various types of pyrometers are considered, and two approaches are presented for obtaining accurate brightness temperature measurements. The first approach consists of correcting the data for effects of extraneous radiation. The second approach employs a variable-wavelength pyrometer in a wavelength region free from such radiation. Experimental data on a charring ablation material obtained with the second approach are presented and compared with data uncorrected for extraneous radiation obtained with a disappearing-filament optical pyrometer and with a total-radiation pyrometer. The results indicate that large amounts of extraneous radiation from the testing environment used are present within the sensitive wavelength regions of the latter two instruments.

An error analysis shows that good accuracy in surface temperature measurements is now well within the state of the art for a variable-wavelength pyrometer. The experimental data show that reproducibility of data obtained with such an instrument is extremely good and that the instrument is highly sensitive to small surface temperature changes.

INTRODUCTION

Part of the evaluation of proposed ablation materials consists of a detailed energy balance of the processes involved in ablation. This is obtained by testing the material in a high velocity gas stream simulating the expected entry environment. An important test parameter is the surface temperature from which the energy radiated is obtained.

At present, the most accurate methods for obtaining surface temperatures of glowing ablation materials are those involving the techniques of optical pyrometry for which the theoretical relations and experimental methods are well documented. (For example, see ref. 1.) These techniques, however, are subject to serious error if extraneous radiation is present. Such radiation may be present in the hot gas streams produced by certain

types of test facilities or may come into the optical path by reflections from the specimen surface.

Two methods for handling extraneous radiation are presented in this paper. The first method consists of identifying and subtracting the portion of total measured radiation which is extraneous. Where the amount of extraneous radiation is small, certain approximate corrections are sufficient as discussed in reference 2. The presence of large amounts of extraneous radiation requires a more rigorous treatment of corrections as presented in appendix A of this paper. Certain types of extraneous radiation may be found impossible to handle with this method of subtracting correction terms.

The second method employs use of a narrow-bandwidth pyrometer with variable wavelength in a portion of the spectrum free from extraneous radiation. Such a method is inherently more accurate than a method requiring a number of corrections, each of which involves some degree of error.

In the work presented herein, this second method is used to obtain experimental data which are compared with data obtained with a disappearing-filament optical pyrometer and a total-radiation pyrometer. The results indicate that large amounts of extraneous radiation from the testing environment used are present within the sensitive wavelength regions of the latter two instruments.

An error analysis shows that good accuracy in surface temperature measurements is now well within the state of the art for a variable-wavelength pyrometer. The experimental data show that reproducibility of data obtained with such an instrument is excellent and that the instrument is highly sensitive to small surface temperature changes.

SYMBOLS

The units used for the physical quantities in this paper are given in the International System of Units (SI). Factors relating this system to the U.S. Customary Units are given in reference 3.

$B_{\lambda}(T)$	effective spectral radiance of source at temperature T emitting line and/or band radiation in addition to any continuum radiation emitted
C_1	first constant in Planck black-body radiation function, 1.1909×10^{-16} watt-meter ² -steradian ⁻¹
C_2	second constant in Planck black-body radiation function, 1.4388×10^{-2} meter-°K

G	gain setting
I	signal intensity
$K(\lambda)$	function used, for convenience, to represent product of series of transmittances and detector spectral sensitivity
L	luminance or photometric brightness
$N_{\lambda}(T)$	spectral radiance (energy emitted from a body at temperature T at wavelength λ per unit time per unit solid angle per unit projected area per unit wavelength interval), watt-meter ⁻² -steradian ⁻¹ -meter ⁻¹
Q	experimental quantity
T	temperature, °K
T_B	brightness temperature (temperature of a black body which has same spectral radiance at a particular wavelength as source (see ref. 1)), °K
V_{λ}	relative spectral sensitivity of detector
P	radiant power, watts/meter ²
X	constant factor
ϵ_{λ}	spectral emittance
θ	angle, radians
λ	wavelength
ρ_{λ}	spectral reflectance
σ	Stefan-Boltzmann constant, $9.024 \times 10^{-9} \frac{\text{watts}}{\text{meter}^2 \cdot (\text{°K})^4 \cdot \text{steradian}}$
τ_{λ}	spectral transmittance

Subscripts:

b	blackbody
BG	background
c	cooled
e	emitted
f	filter
i	incident
pc	primary calibration
r	reflected
s	specimen
sc	secondary calibration
t	test specimen
1,2,3,...	numbers used to differentiate between luminances and temperatures

Superscripts:

'','',''	used to differentiate between transmittances, gain setting, signal intensities, etc.
----------	--

APPARATUS AND TEST SPECIMENS

Test Facility

The radiating test medium was provided by the 2.5-megawatt atmospheric arc jet at the Langley Research Center. As with all facilities of this type, the hot gas stream is produced by passing the gas through a region containing electric arcs. The gas is heated by the arcs, then proceeds subsonically through a nozzle, and is ejected to the atmosphere. A more complete description of this particular facility is given in reference 4.

Test Models

The ablation models tested were all in the form of flat-face 7.6-cm-diameter cylinders and with lengths varying from 2.0 to 2.2 cm. The material used, a charring ablator with a density of approximately 1.2 Mg/m³, was a homogeneous mixture of 50 percent (by weight) nylon powder and 50 percent phenolic resin powder.

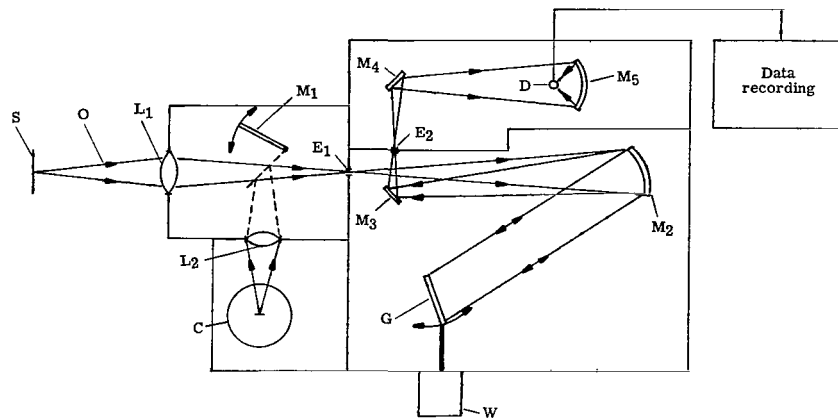
In addition, several tests were made on a graphite model whose front surface had been coated to a depth of about 0.8 cm with pyrolytic graphite. This model was a flat-face 7.6-cm-diameter cylinder approximately 10 cm long.

Pyrometers

Two pyrometers were used to obtain surface brightness temperatures. The first was a disappearing-filament optical pyrometer used to obtain data uncorrected for extraneous radiation. As the name suggests, this pyrometer operates by focusing the image from a source on the plane of a calibrated lamp filament then adjusting the filament current until the filament luminance matches that of the source. This pyrometer has a fixed wavelength with a band pass ranging from approximately 0.62 μm to 0.72 μm depending upon the relative luminosity factor of the observer. (See ref. 1.) The mean effective wavelength (ref. 1) of this instrument is, nominally, 0.653 μm . The disappearing-filament pyrometer is calibrated by means of a tungsten-filament lamp which has, in turn, been calibrated by the National Bureau of Standards.

The second pyrometer was an instrument designed for determination of gas temperatures by using emission and absorption measurements. (See ref. 5.) It consists basically of a monochromator with the variable-wavelength adjustment presently calibrated in the range 1.0 to 3.0 μm and with a built-in tungsten filament lamp used as a secondary energy calibration. (See fig. 1 for schematic diagram.) A commercially produced blackbody is used to obtain a primary energy calibration. The lead sulfide energy detector temperatures are in the range of 290° to 300° K, stabilized to within $\pm 0.10^\circ$ K for testing times used. The detector signal is amplified, then recorded as a function of time on a strip-chart recorder.

Entrance and exit slits are equal in width and six different fixed widths varying from 1.00 to 0.025 mm are provided. This gives wavelength bandwidths of 24.7 to 0.617 nm for radiation at a wavelength of 1.00 μm and 22.3 to 0.557 nm at a wavelength of 3.00 μm .



S	Source
O	Optical path
L ₁	Source focusing lens
M ₁	Two-position plane mirror (brings energy from secondary-calibration lamp into optical path)
L ₂	Secondary-calibration-lamp focusing lens
C	Secondary-calibration lamp
E ₁	Entrance slit (multiple fixed widths)
M ₂	Off-axis paraboloid mirror
G	Plane reflection grating
W	Wavelength drive (scans wavelength by rotating grating)
M ₃ , M ₄	Fixed plane mirrors
E ₂	Exit slit (multiple fixed widths)
M ₅	Spherical mirror (focuses energy onto detector)
D	Detector

Figure 1.- Schematic of optical system of variable-wavelength pyrometer with internal energy-calibration lamp.

METHODS AND EXPERIMENTAL PROCEDURES FOR HANDLING EXTRANEOUS RADIATION

The basic equations used in the theory of optical pyrometry are well covered in the literature (e.g., ref. 1); thus, they are not discussed herein. For convenience, they are summarized briefly in appendix B.

If the radiation entering an optical pyrometer is emitted only from the real body under observation, accurate surface temperatures are readily obtained. However, if extraneous radiation is present, the observed luminance and corresponding surface temperatures are increased in proportion to the amount of such radiation. It is then necessary either to correct the measured luminance for the effects of extraneous radiation or, if the radiation is in the form of atomic or molecular lines or bands, to make measurements in a wavelength region free from it. A combination of these two methods may be necessary if the extraneous radiation consists of both a continuum and atomic or molecular lines or bands. Consider, for example, the spectrograms, reproduced in figure 2, which were made of the gas stream of the arc-jet facility used in this study. In addition

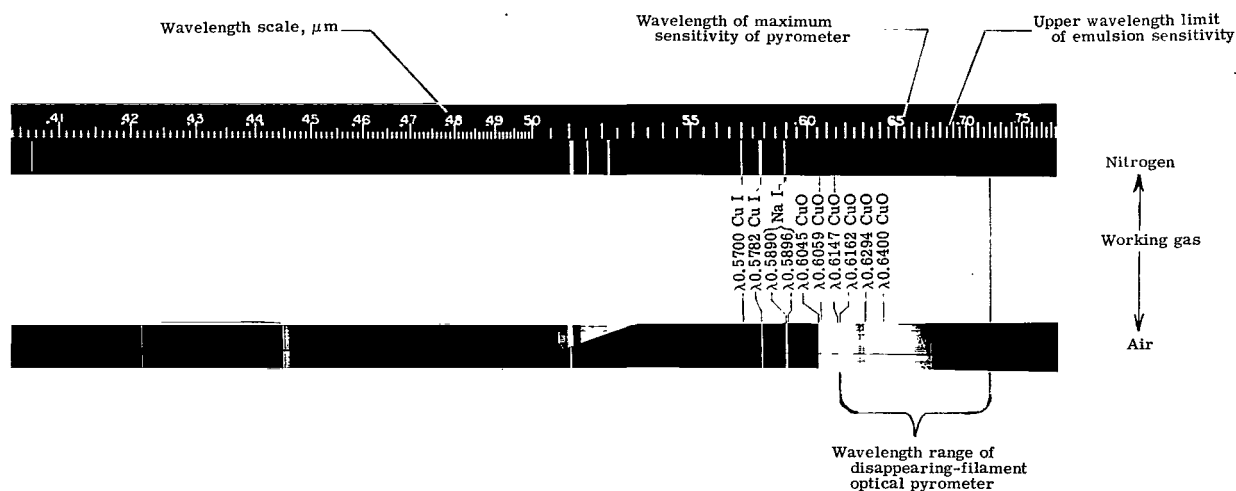


Figure 2.- Spectrums of gas stream of 2.5-megawatt atmospheric arc jet at Langley Research Center on type 103-F emulsion.

to the line and band structure apparent, an underlying continuum shows up in microdensitometer traces. If a variable-wavelength pyrometer were to be used in making brightness temperature measurements of specimens in a facility of this type, one would pick a wavelength region where the total extraneous radiation is a minimum. The luminance due to unavoidable extraneous radiation would then be determined and subtracted from the total measured luminance. This procedure minimizes errors due to uncertainties in measurement of correction terms.

In order to serve as a guide for experimenters restricted to use of fixed-wavelength instruments, a fairly rigorous treatment of a method for obtaining the spectral radiance of a test specimen in the presence of extraneous radiation by subtraction of correction terms is presented in appendix A. Use of this method, however, requires prior knowledge of the directed spectral reflectances of the test and calibration specimen surfaces and of the spatial distribution of extraneous radiation emitted from the gaseous testing environment. Aside from the fact that each of these correction terms contains its own inherent experimental error, the necessary reflectance data are only rarely found in the literature and even then are often contradictory from one source to another. This necessitates setting up an independent reflectance measuring experiment, a tedious and difficult process in itself, if meaningful and reliable data are to be obtained.

A further examination of this method reveals that it does not account for the possibility of radiation from the gaseous products of the ablation process. In fact, a method of correcting for radiation from these outgassing ablation products is not immediately

apparent and, if not impossible, will certainly be difficult and will contain yet another inherent experimental error.

For these reasons, a method of obtaining test specimen luminance* by means of a variable-wavelength instrument has been considered and experimentally tested. In this method, the radiation from the test specimen and testing environment are surveyed separately as a function of wavelength, following which a wavelength region free of extraneous radiation is used for a luminance measurement. Corrections for extraneous radiation are thus eliminated and both the spectral radiance and temperature of the specimen are easily calculated by means of the basic pyrometer relationships. In order to serve as a guideline or point of departure for other experimenters, the experimental procedures used in this study are given in detail as follows.

With the specimen in testing position, the pyrometer was focused on the center of the test specimen. Because of the geometry of the test setup, an observation angle of about 70° from the normal to the surface of the specimen was used. The setting-up procedure included checking for and eliminating any sources of background radiation, such as illumination lamps for photographic data recording, both with and without the specimen in testing position.

The arc jet was then turned on with the specimen removed from the testing position and the pyrometer wavelength scan was activated. This resulting strip-chart recording gave a curve of arc-jet emission as a function of wavelength over the instrument calibrated wavelength range. The use of both air and nitrogen as test gases required performing this procedure for each test gas. The absence of measurable emission from the test gas over the calibrated range of the pyrometer allowed measurements to be made at any desired wavelength within the calibrated range. If strong emission had been present in some wavelength regions, these regions would have been avoided during the subsequent testing.

Next a test specimen was placed in the testing position with the arc jet on and the pyrometer wavelength-acceptance band was again scanned over the calibrated wavelength region. The data obtained in this step were used to determine the existence of line or band radiation emitted by the gases effluent from the ablating test specimen. Such radiation would show up on the strip-chart recording as "blips" in the shape of line or band

*Luminance is defined in the literature as the radiance of a surface evaluated according to its capacity to produce visual sensation. (See ref. 1.) The definition is extended in this paper to include detectors other than the human eye — that is, photoelectric or thermoelectric detectors; hence, also included are wavelengths outside the human visual range. This extension is valid since the mathematical description for luminance holds for automatic detectors as well as for the human eye.

profiles superimposed upon the continuum radiation from the specimen. Again, such radiation was not found. Its presence over some given wavelength region would have necessitated avoiding that region in making the final luminance measurements.

Finally, with the pyrometer wavelength fixed at $1.0\ \mu\text{m}$, a measurement was made of the luminance of the test specimen as a function of testing time. These data were then reduced to obtain spectral radiance and brightness temperature as a function of time by use of the basic pyrometer relationships.

For comparison purposes, simultaneous measurements with a standard, disappearing-filament, optical pyrometer were made for several tests. As with the variable-wavelength pyrometer, the geometry of the test setup necessitated a look angle of 70° to 80° from the normal to the test specimen surface. The pyrometer was focused initially on the center of the test specimens, but difficulty in focus position was encountered during the testing periods because of a tendency to seek local hot spots rather than the center.

PRECISION

Minimizing experimental error is of particular importance in projects of this type where the data obtained are merely one of many terms in a complicated energy balance equation for an ablation material. Hence, a formal estimate of experimental error is necessary to obtain an indication of the reliability of data and to determine which error sources are most important.

The requirements both for a high degree of precision and for time- and space-resolved measurements necessitate the use of automatic data-recording instruments rather than those which use the human eye as a detector. These instruments not only eliminate the possible human error but also allow the use of much narrower spectral bandwidths; hence, the error due to uncertainty in wavelength is decreased.

The accuracy required also makes desirable the use of monochromatic rather than total-radiation pyrometers or multiwavelength instruments, especially if fixed-wavelength instruments are used. This is because of the greater inherent accuracy of the monochromatic instruments for laboratory use (ref. 6) plus the possibility of much greater error in the total radiation pyrometer or the multiwavelength instruments due to effects of extraneous radiation, particularly if the majority of the extraneous radiation is concentrated in only one of the sensitive wave bands of the multiwavelength instruments.

Error Analysis for Automatic Pyrometer

In the actual measurements made with a narrow-bandwidth optical pyrometer, the spectral radiance $N_{\lambda,b}(T_B)$ of a source at a brightness temperature T_B is obtained from the proportionality

$$N_{\lambda,b}(T_B) \propto I_t \quad (1)$$

where I_t is the recorded test specimen signal. If a null-balancing data-readout method is used, such as with a disappearing-filament pyrometer, the source radiance is equal to that of the calibration lamp and the source brightness temperature is obtained directly from the lamp's calibration curve. When the instrument used does not operate by a null-balancing technique but instead on the assumption that the output signal is directly proportional to the intensity of the input radiation, the specimen spectral radiance is given by

$$N_{\lambda,b}(T_B) = \frac{G_{sc}}{G_t} \frac{I_t}{I_{sc}} N_{\lambda}(T_1) \quad (2)$$

where, for the instrument of interest in this report, the radiance from the internal secondary energy calibration lamp $N_{\lambda}(T_1)$ is a constant since the lamp current is held constant. If different gain settings are used for the test specimen and calibration signals, the ratio of signal intensities I_t/I_{sc} must be multiplied by the ratio of gain settings G_{sc}/G_t . Also, both the signal-intensity and gain-setting ratios must be corrected for any nonlinearities present.

The primary calibration of the instrument by means of a black body at known temperature results in an equation similar to equation (2) for the secondary calibration radiance $N_{\lambda}(T_1)$. In terms of the primary calibration, then, the test specimen spectral radiance is

$$N_{\lambda,b}(T_B) = \frac{G_{sc}}{G_t} \frac{I_t}{I_{sc}} \frac{G_{pc}}{G'_{sc}} \frac{I'_{sc}}{I_{pc}} N_{\lambda,b}(T_{pc}) \quad (3)$$

where the primes are used to differentiate between the signal intensity and gain setting of the secondary calibration lamp for the primary calibration (I'_{sc} and G'_{sc}) and for the test run (I_{sc} and G_{sc}). If the Planck black-body radiation function as given by equation (B2) is used for the spectral radiance of the primary-calibration black body $N_{\lambda,b}(T_{pc})$, the following expression for the spectral radiance of the test specimen is obtained:

$$N_{\lambda,b}(T_B) = \frac{G_{sc}}{G_t} \frac{I_t}{I_{sc}} \frac{G_{pc}}{G'_{sc}} \frac{I'_{sc}}{I_{pc}} \frac{C_1}{\lambda^5} \left[\exp\left(\frac{C_2}{\lambda T_{pc}}\right) - 1 \right]^{-1} \quad (4)$$

When this expression is used, the mathematical expression for the experimental uncertainty of $N_{\lambda,b}(T_B)$ is obtained by the standard procedure (ref. 7) of taking the total derivative of the logarithm of equation (4), then passing from the infinitesimal derivatives to finite intervals for which the corresponding individual error estimates are substituted in the application of the equation. The most probable experimental error in the spectral radiance of a test specimen, defined as the square root of the sum of the squared error

terms, is given by

$$\frac{\Delta N_{\lambda,b}(T_B)}{N_{\lambda,b}(T_B)} = \left\{ \left[\frac{\Delta(G_{sc}/G_t)}{G_{sc}/G_t} \right]^2 + \left[\frac{\Delta(G_{pc}/G'_{sc})}{G_{pc}/G'_{sc}} \right]^2 + \left(\frac{\Delta I_t}{I_t} \right)^2 + \left(\frac{\Delta I'_{sc}}{I'_{sc}} \right)^2 + \left(\frac{\Delta I_{sc}}{I_{sc}} \right)^2 + \left(\frac{\Delta I_{pc}}{I_{pc}} \right)^2 + \left(\frac{C_2}{\lambda T_{pc}} - 5 \right)^2 \left(\frac{\Delta \lambda}{\lambda} \right)^2 + \left(\frac{C_2}{\lambda T_{pc}} \right)^2 \left(\frac{\Delta T_{pc}}{T_{pc}} \right)^2 \right\}^{1/2} \quad (5)$$

where the uncertainties in the constants C_1 and C_2 of the Planck black-body radiation law are considered negligible and it is assumed that the wavelength is small enough (i.e., $\lambda < 2.5 \mu\text{m}$) to make the one in the term containing an exponential function of equation (4) negligible in comparison with the exponential. This allows cancellation of the exponential functions and equation (5) results.

Writing equation (B7) in terms of a temperature T rather than T_2 and applying the procedure just outlined, one obtains a most probable error in the spectral radiance of a black body of temperature T of

$$\frac{\Delta N_{\lambda,b}(T)}{N_{\lambda,b}(T)} = \left\{ \left[\frac{\Delta N_{\lambda,b}(T_B)}{N_{\lambda,b}(T_B)} \right]^2 + \left[\frac{\Delta \epsilon_{\lambda}(T, \theta)}{\epsilon_{\lambda}(T, \theta)} \right]^2 \right\}^{1/2} \quad (6)$$

From equation (6) the probable error in the true temperature of the specimen is (using eq. (B2) for $N_{\lambda,b}(T)$):

$$\frac{\Delta T}{T} = \frac{\lambda T}{C_2} \left\{ \left[\frac{\Delta N_{\lambda,b}(T_B)}{N_{\lambda,b}(T_B)} \right]^2 + \left[\frac{\Delta \epsilon_{\lambda}(T, \theta)}{\epsilon_{\lambda}(T, \theta)} \right]^2 + \left(5 - \frac{C_2}{\lambda T} \right)^2 \left(\frac{\Delta \lambda}{\lambda} \right)^2 \right\}^{1/2} \quad (7)$$

Equations (5) and (7) have been used to obtain a most probable estimated error for a test case of $T = 2000^\circ \text{K}$ and $\lambda = 1.00 \mu\text{m}$ for the instrument used in this experiment. The results as well as the intermediate error estimates are presented in table I. The estimate of each contributor to the total error is either experimentally determined, estimated from a knowledge of the quantities involved, or arrived at by some combination of these two. The source of each estimated uncertainty is indicated in the last column. Most of the estimated uncertainties have been made deliberately large in an attempt to account for any overlooked error sources.

The same equations can be applied to an instrument now possible at the present state of the art by estimating that the uncertainties in the gain linearities G_{sc}/G_t and G_{pc}/G'_{sc} are ± 1 percent, and that the uncertainties in the terms I'_{sc} , I_{sc} , and I_t are all ± 2.2 percent (± 0.2 percent reading error plus 1 percent linearity error plus 1 percent

TABLE I.- ESTIMATE OF MOST PROBABLE EXPERIMENTAL ERROR FOR A
VARIABLE-WAVELENGTH MONOCHROMATIC RADIATION PYROMETER

Quantity, Q	Estimated uncertainty, $\frac{\Delta Q}{Q}$	Source of uncertainty estimate
G_{sc}/G_t	0.036	Average of several experimental measurements
G_{pc}/G'_{sc}	0	Identical gain setting, hence zero uncertainty
I_{pc}	0.012	<div style="display: inline-block; vertical-align: middle; font-size: 3em; line-height: 1;">}</div> Reading error (estimated within ± 0.2 division on a 100-division scale) Linearity error (estimated within ± 1 percent) Errors due to instrument instabilities (estimated up to ± 30 percent)
I'_{sc}	0.112	
I_{sc}	0.312	
I_t	0.112	
T_{pc}	0.010	Estimated
λ	0.005	Wavelength setting uncertainty (estimated) Calculated uncertainty due to instrument spectral slit width
$\epsilon_\lambda(T, \theta)$	0.20	Estimated
$N_{\lambda, b}(T_B)$	0.372	Equation (5)
$N_{\lambda, b}(T)$	0.422	Equation (6)
T_B	0.052	Equation (7)
T	0.059	

uncertainty due to instrument instabilities). All other terms are estimated as given in table I. Using these values, it is found that uncertainties in brightness temperatures of 1 percent or less rather than the minimum of 5 percent with the present instrument are attainable. Hence, for an instrument possible at the present state of the art, the uncertainty in directed spectral emittance is the dominant source of error in true surface temperatures.

RESULTS AND DISCUSSION

As outlined in the introduction, energy radiated from the glowing surface of an ablation material under test is an important component of the energy balance equation for such a material. First attempts in this facility to obtain radiated energy were made by applying surface brightness temperatures measured with a standard disappearing-filament optical pyrometer to the familiar Stefan-Boltzmann law:

$$P = \epsilon \sigma T^4 \quad (8)$$

where σ is the Stefan-Boltzmann constant and the total emittance ϵ was assumed to be unity.

The temperatures obtained in these preliminary measurements indicated, however, that the ablation specimens were radiating more energy than the energy input to them as measured by a cold-wall calorimeter.

Since the uncertainties in calorimetrically measured energy inputs were suspected to be less than the indicated discrepancies, the accuracy of data obtained with the disappearing-filament optical pyrometer was questioned. Confirmation of the calibration of the optical pyrometer indicated the possibility of errors as a result of extraneous radiation from the testing environment.

Portions of spectrographic plates made previously of the gas stream of the arc-jet facility used are given in figure 2. This figure shows the presence of strong line and band radiation throughout the spectral range to which the disappearing-filament optical pyrometer is sensitive. Microdensitometer traces of these spectrum plates show an underlying continuum radiation as well as the band and line radiation apparent to the eye. As might be expected, the strong copper-oxide bands present with air as a working gas are much weaker in the pure nitrogen test stream.

High-speed films of ablation material tests gave further indication of the presence of strong extraneous radiation. Several such films showed, very distinctly, images of the rotating arcs within the arc-jet facility reflected from certain types of glassy-surface ablation materials. Such radiation from within the arc jet could conceivably contribute to the measured luminance of a charring ablation material by means of diffuse reflections from the surface of the specimen.

The first set of data obtained in this study was for the purpose of comparison of the various instruments used in surface temperature measurements. Models and arc-jet test parameters identical to those for which data are presented in reference 8 (specimen 25 in fig. 8) were used. Data obtained both with the variable-wavelength instrument and the disappearing-filament optical pyrometer were compared with the total-radiometer data of reference 8. The results of the comparison, showing brightness temperature as a function of time, are given in figure 3, which includes the data given in reference 8. An indication of the reproducibility of data obtained with the variable-wavelength pyrometer may be found in this figure since the data plotted for that instrument represent measurements made on two separate specimens whose test parameters were as nearly the same as possible. Except for the first few seconds of each test, the reproducibility throughout the test period is so good that the largest percent difference in measured brightness temperature for the two tests is only 0.67 percent.

To examine more closely the discrepancies shown among the three instruments, consider figure 3, for example, at a testing time of 50 sec. If the directed spectral

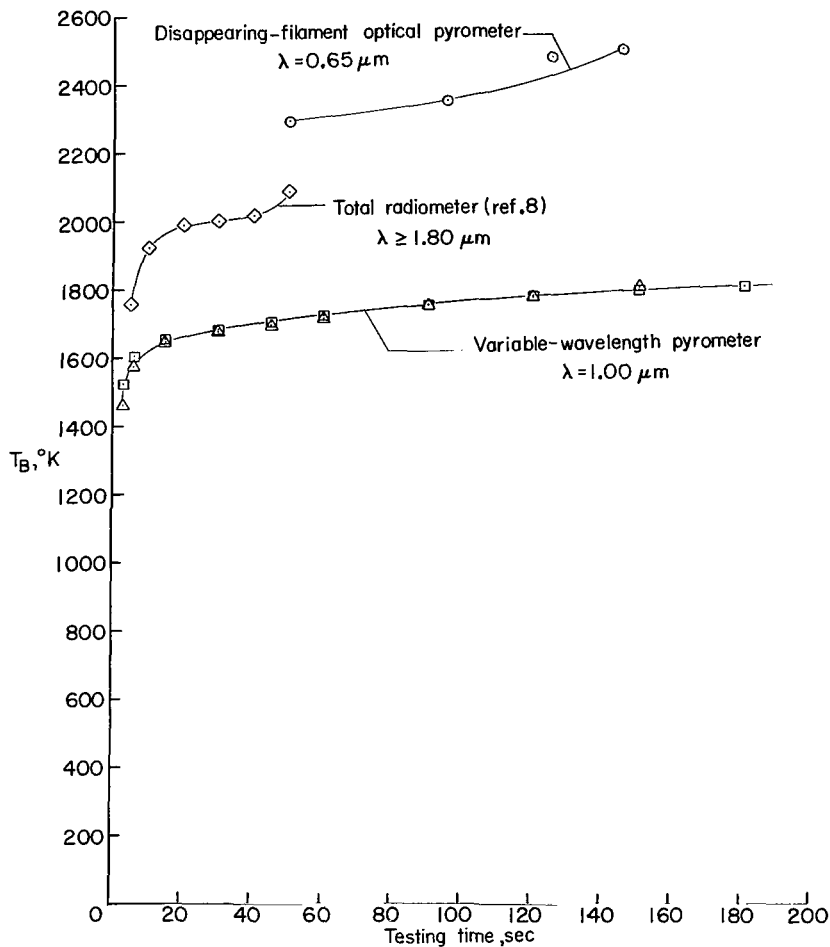


Figure 3.- Comparison of surface-brightness-temperature history of ablation material specimen obtained with different type instruments.

emittance of the specimen is assumed constant over the wavelength range from $0.65 \mu\text{m}$ to $1.00 \mu\text{m}$, the brightness temperature measured by the disappearing-filament optical pyrometer at $0.65 \mu\text{m}$ is the same as would be measured at a wavelength of $1.00 \mu\text{m}$. Then, according to equation (8), the radiated energy rate as calculated from data obtained with the disappearing-filament optical pyrometer is over three times that indicated by the variable-wavelength monochromator. Similarly, the total-radiometer data show a rate of energy emission over two times that indicated by the variable-wavelength monochromator.

Since these differences are somewhat larger than were expected, other possible causes were considered. First, the assumption of constant directed spectral emittance over the wavelength region of interest is probably not valid. Unfortunately, spectral emittance data for the ablation material used has not been available in the literature for the spectral range of interest. If the material is assumed to exhibit a general decrease

in spectral emittance with wavelength similar to that of its main constituent, carbon (as shown in ref. 9), then a linear extrapolation of the data of reference 10 shows the spectral emittance at $1.00\ \mu\text{m}$ is, at most, only about 10 percent less than at $0.65\ \mu\text{m}$.

However, in order to account fully for the differences obtained it would be necessary for the spectral emittance to decrease by at least 80 percent between $0.65\ \mu\text{m}$ and $1.00\ \mu\text{m}$. Therefore, a variation of directed spectral emittance with wavelength apparently does not account for the differences noted.

Calibration error is the second possible cause of the differences in temperatures measured by the various instruments. The calibrations of both the disappearing-filament optical pyrometer and the total radiometer were checked and confirmed. The variable-wavelength monochromator was carefully calibrated just before the tests of figure 3. If the measured spectral radiance is assumed to be low due to calibration error of this instrument, then, when it is adjusted by the estimated 37 percent most probable error, the radiated energy rate obtained with the disappearing-filament optical pyrometer is still 2.8 times that indicated by the variable-wavelength monochromator. If the estimated 10-percent decrease in directed spectral emittance between the wavelength of $0.65\ \mu\text{m}$ and $1.00\ \mu\text{m}$ is included, the ratio of measured energy emission rates for the two instruments is 2.6, and the ratio obtained with the total radiometer to the adjusted rate measured with the variable-wavelength monochromator is 1.9.

These differences are still so much larger than expected that some unknown source of error in the calibration of one or more of the instruments cannot be discounted. In addition, there exists the possibility of error due to interference from the large fluctuating electric and magnetic fields in the vicinity of the arc-jet facility in which tests were made. Particular care was taken in placement of the variable-wavelength pyrometer for these tests in an attempt to avoid such interference, and it was noted that the starting and running of the arc jet caused no measurable deflection of the strip-chart recorder. However, the absolute accuracy of these particular measurements is not of importance here, as they are being used mainly to illustrate the proper methods to use for obtaining surface temperatures in the presence of large amounts of extraneous radiation. The large differences obtained in the comparison certainly indicate a strong possibility that extraneous radiation is indeed affecting the measurements made with the disappearing-filament optical pyrometer.

Additional tests made with a pyrolytic graphite specimen give further indications of the sensitivity of measurements made with this type of instrument. The data presented in figure 4 show the effect on surface temperature of changing input heating rate and working-gas composition. These tests were all done on the same specimen since the heating rates used were too low to ablate the pyrolytic graphite surfaces. As expected, the surface temperature increases with increased heating rate and the small changes of

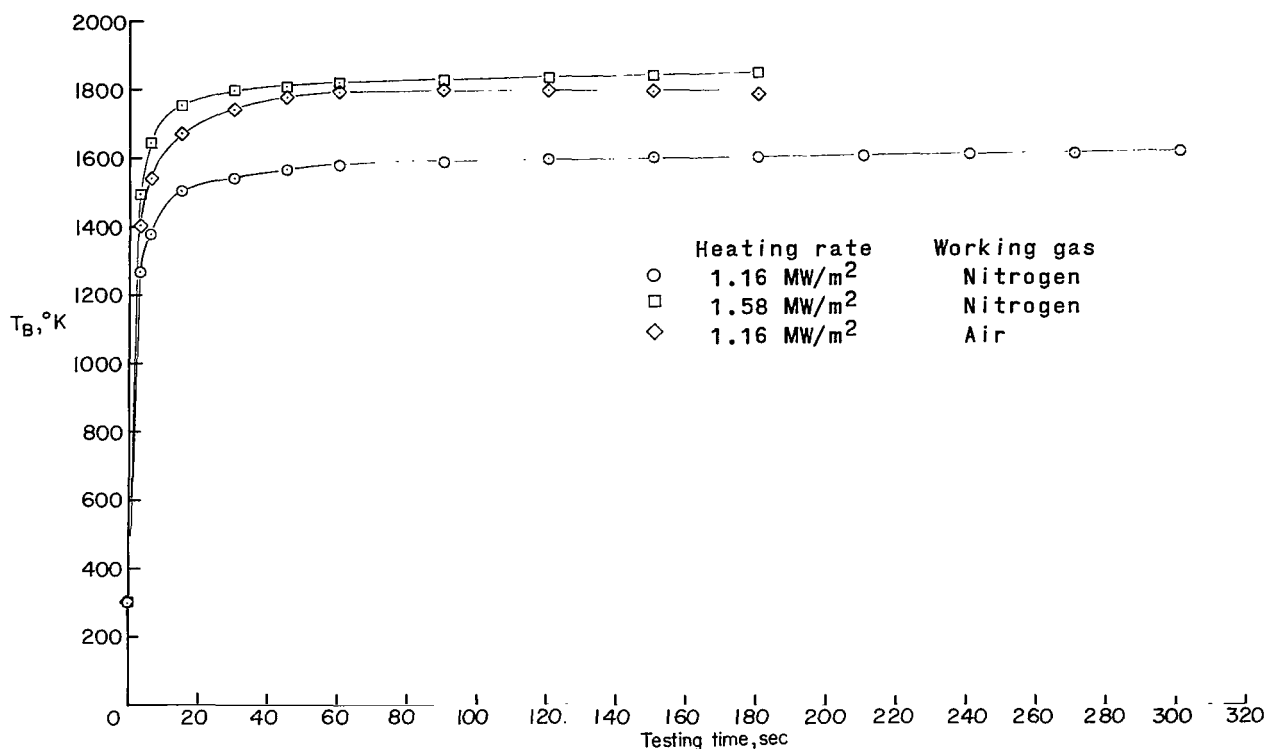


Figure 4.- Effects of surface heating rate and test gas composition on brightness temperature of pyrolytic graphite specimen as measured by variable-wavelength pyrometer.

temperature during the test runs by the variable wavelength pyrometer are easily detected. Also, the addition of oxygen to the working gas increases the surface temperature because of catalytic and oxidation effects at the model surface.

POSSIBILITIES FOR FUTURE DEVELOPMENT

In addition to the accuracy (see section "Precision"), sensitivity, and reproducibility possible with the variable-wavelength type of instrument, several other possible future applications are well worth considering.

First, the output data signal, available as a small varying voltage, need not be recorded on a strip-chart. Much data-reduction time can be easily eliminated by recording on tape or by some other method easily adaptable to computerized data reduction. Only those constants necessary for calibration are required, in addition to the recorded data, for automatic data reduction.

Second, the external optics of the instrument can be designed to provide rapid scanning of the test specimen image across the entrance slit of the monochromator. This,

coupled with automatic recording and data reduction, can result in space-resolved as well as time-resolved surface-brightness-temperature histories of test specimens.

Finally, rather than employ a monochromator, a multiwavelength instrument, for which each wavelength region can be independently adjusted to avoid extraneous radiation, could be used. With data from such an instrument, two-or-three-color pyrometry theory (ref. 6) could be applied to obtain a rough first approximation for a true surface temperature. The data from each wavelength channel could then be used to obtain brightness temperatures from which relative emittances could be calculated. These relative emittances could be used in the multicolor theory to obtain second approximations to surface temperatures. By iterating (assuming that the iteration converges), it should be possible to obtain not only true surface temperatures but also relative spectral emittance over the wavelength range covered by the several wavelength channels being recorded. A knowledge of emittance at some particular wavelength for a given temperature could then result in absolute emittances at several wavelengths as a function of measured surface temperatures.

CONCLUDING REMARKS

Extraneous radiation has been found present in the testing environment of the 2.5-megawatt atmospheric arc jet at the Langley Research Center. A comparison of ablation specimen surface temperatures obtained with three different types of pyrometer indicates that the presence of such radiation may seriously affect measurements. The preferred method for handling extraneous radiation is by use of a variable-wavelength, narrow-bandwidth pyrometer in spectral regions free of such radiation. Such an instrument is extremely sensitive to small temperature changes and provides data highly reproducible from test to test.

Langley Research Center,
National Aeronautics and Space Administration,
Langley Station, Hampton, Va., March 3, 1966,
124-08-03-13-23.

APPENDIX A

METHOD FOR CORRECTING LUMINANCE MEASUREMENTS FOR THE PRESENCE OF EXTRANEEOUS RADIATION

A fairly thorough literature search has shown an apparent lack of a rigorous treatment of a method for correcting for extraneous radiation. This appendix is an attempt to correct such a lack. It is general enough to be applicable both to the standard disappearing-filament type optical pyrometer and to more sophisticated variable-wavelength instruments with automatic data detection and recording.

In order to make the required corrections for extraneous radiation, it is necessary to assume that any extraneous line or band radiation falling within the sensitive wavelength band of the instrument will cause the same detector response as that caused by a black body at some given temperature. It is then valid to treat the total measured luminance as the sum of the luminances from the test specimen and from one or more "effective" black bodies representing extraneous radiation. Luminance is defined in the literature as the radiance of a surface evaluated according to its capacity to produce visual sensation but it is extended in this paper to include detectors other than the human eye — that is, photoelectric or thermoelectric detectors; hence, also included are wavelengths outside the human visual range.

Sources of Extraneous Radiation

The possible sources of extraneous radiation considered here are background radiation from the general environment around the test facility, radiation emitted from the immediate testing environment, and radiation reflected from the test specimen.

The first may occur as direct or reflected radiation from sources or reflective surfaces intruding into the solid angle of the pyrometer optical path. Proper pyrometer placement or careful shielding will usually eliminate such radiation. The possibility that it cannot be eliminated necessitates considering two contributors to background radiation. The first contributor is radiation originating within the portion of the pyrometer optical path extending beyond the model position; this radiation does not enter the pyrometer when the model is in position. Background radiation entering the optical path between the pyrometer and the specimen testing position is not considered since it can almost always be eliminated by proper pyrometer placement. The first contributor to background radiation causes a detector response of luminance L_{BG} . Reflections from the specimen surface comprise the second contributor to background radiation. The resulting luminance is included in another reflection term to be considered later.

APPENDIX A

Radiation emitted from the immediate testing environment, such as from the hot gases surrounding a specimen in an arc-jet stream, consists of line or band radiation and, possibly, of continuum radiation. This radiation is measured as a luminance L_e .

The radiation reflected from the test specimen surface can originate from either the immediate or the general testing environment. The measured reflected luminance $L_{r,s}$ includes the reflections due to the background radiation discussed previously.

The total measured luminance of a test specimen surface is expressed mathematically as

$$L = L_e + L_{r,s} + L_s \quad (A1)$$

where L_s is the luminance of the test specimen at a brightness temperature of T_B .

Isolation of Correction Terms

The luminance of the test specimen is obtained by isolating in a stepwise fashion the various contributors to extraneous radiation and subtracting their luminances from the total measured luminance.

When the pyrometer has been positioned and focused, the first measurement is made with the testing facility not operating and the test specimen not in the optical path of the instrument. This gives a value for background luminance L_{BG} originating along the portion of the optical path of the instrument extending beyond the specimen position, as shown in figure 5(a).

The next measurement is made with the testing facility operating but again with the test specimen not in testing position. The measured luminance in this step is the sum $L_{BG} + XL_e$, and, since L_{BG} has been determined, XL_e is readily obtained. (See fig. 5(b).) The factor X is used to indicate that only a portion of the total radiation measured along the unobstructed optical path is present with a specimen in position. This factor is 2 for the ideal case (see path I in fig. 5(b)) of an optical path perpendicular to the axis of a cylindrically symmetrical test stream and with the stream axis as the pyrometer focal point. In general, however, test-facility geometries and specimen positions do not permit this ideal condition; the optical path is as indicated by path II of figure 5(b). Thus, because of axial as well as radial gradients of radiation intensity within the test stream, a factor of 2 for X will give only a crude approximation to the correct value of L_e . A better approximation may be obtained by applying the Abel inversion technique (ref. 11) at a sufficient number of axial positions in the gas stream to allow determination of the relative intensity profile along the unobstructed optical path. The factor X is obtained from a plot of relative intensity against distance along the optical path by taking the ratio of the area under the portion of the curve resulting from radiation between the pyrometer and the model position to the total area. Unless preliminary measurements

APPENDIX A

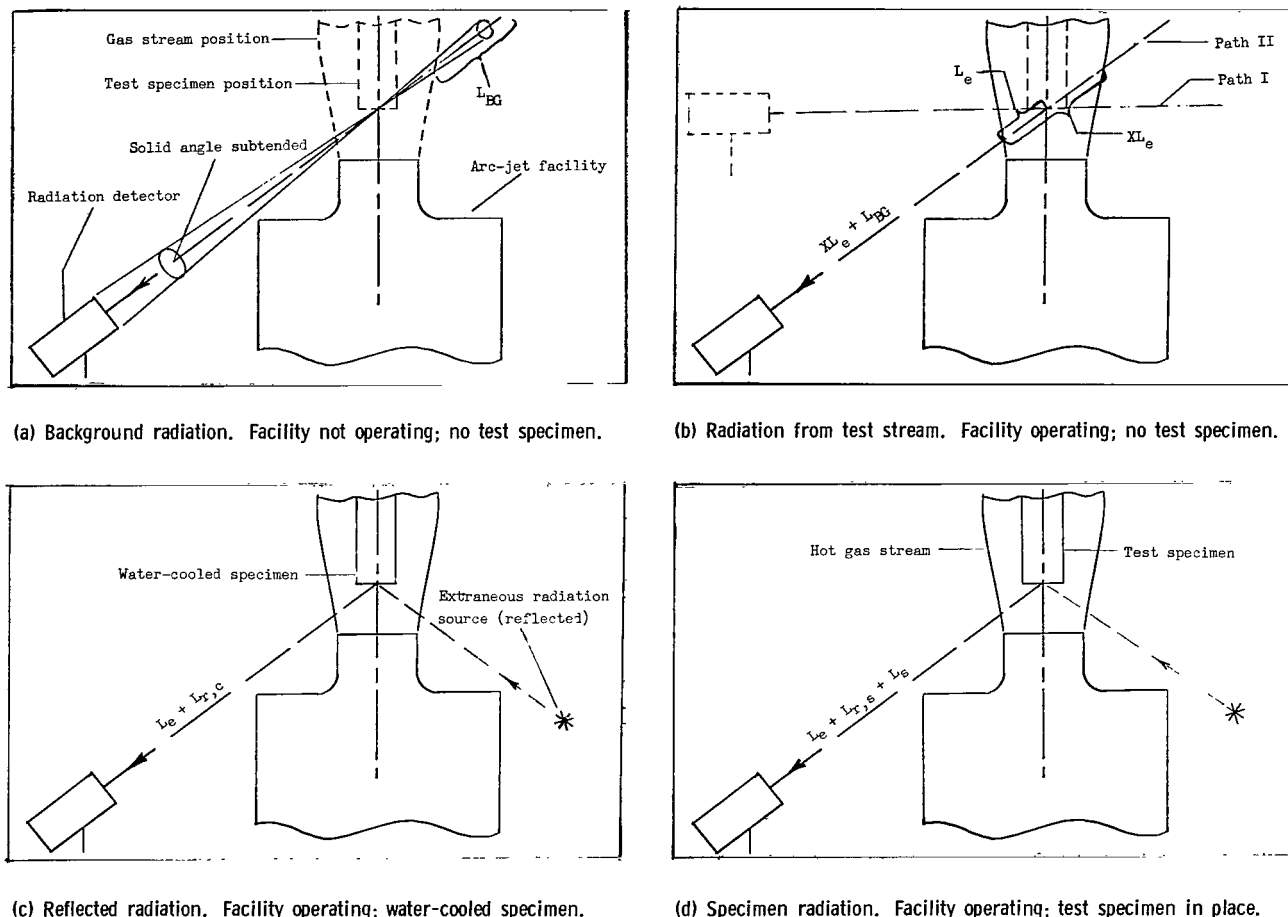


Figure 5.- Schematic of method for step-by-step isolation of correction terms for extraneous radiation.

show that the luminance of the test gas is a large portion of the total measured luminance and that an extremely unsymmetrical intensity profile along the optical path exists, the time and effort required to obtain an approximation to the factor X better than 2 is unwarranted.

The third measurement is made with the test facility operating and with a metal water-cooled specimen of the same size as the ablation specimen in the testing position as shown in figure 5(c). The cooling insures that no detectable radiation is emitted from the specimen itself; hence, reflected radiation can be isolated. The measured luminance L_1 is given by the sum

$$L_1 = L_e + L_{r,c} \quad (A2)$$

where the luminance reflected from the cooled specimen $L_{r,c}$ includes sources both in the immediate testing environment (such as from the arcs within the arc-jet facility) and from the background.

APPENDIX A

The last measurement is made with the test facility operating and the test specimen in position. (See fig. 5(d).) The measured luminance is that expressed by equation (A1).

Reflectance Corrections

In order to determine the luminance of the test specimen L_s , it is necessary to correlate the terms for reflected luminance $L_{r,s}$ and $L_{r,c}$ in equations (A1) and (A2). These luminances are not equal, except by coincidence, because of the differences in temperature and directed spectral reflectance between the water-cooled and the radiating test specimens.

A specimen with a perfectly reflecting surface would result in a measured luminance L_i independent of specimen surface properties. The integral representations for L_i and for the actual measured luminances $L_{r,c}$ and $L_{r,s}$ are written:

$$\left. \begin{aligned} L_i &= \int_0^\infty B_{\lambda,i}(T_3) K_1(\lambda) d\lambda \\ L_{r,s} &= \int_0^\infty B_{\lambda,r,s}(T_4) K_1(\lambda) d\lambda \\ L_{r,c} &= \int_0^\infty B_{\lambda,r,c}(T_5) K_1(\lambda) d\lambda \end{aligned} \right\} \quad (A3)$$

where the various B_λ terms are radiance terms which include the effects of the spectral distribution of the extraneous radiation. The temperatures (T_3 , T_4 , and T_5) differentiate between the effective temperatures of the effective black bodies producing the various luminances in question. The relations between the integral representations for L_i and $L_{r,s}$ and $L_{r,c}$ are given by

$$\int_0^\infty \rho_\lambda(T, \theta) B_{\lambda,i}(T_3) K_1(\lambda) d\lambda = \int_0^\infty B_{\lambda,r,s}(T_4) K_1(\lambda) d\lambda \quad (A4)$$

and

$$\int_0^\infty \rho_\lambda(T_6, \theta) B_{\lambda,i}(T_3) K_1(\lambda) d\lambda = \int_0^\infty B_{\lambda,r,c}(T_5) K_1(\lambda) d\lambda \quad (A5)$$

APPENDIX A

where $\rho_\lambda(T, \theta)$ and $\rho_\lambda(T_6, \theta)$ are the spectral reflectances of the radiating test specimen at temperature T and the water-cooled specimen at temperature T_6 , respectively, as observed at an angle θ from the normal to the surface of each specimen. If the sensitive spectral bandwidth of the pyrometer is narrow enough, these reflectances are closely approximated by constants and, hence, can be taken from under the integral sign to obtain

$$\rho_\lambda(T, \theta) L_i = L_{r,s} \quad (A6)$$

and

$$\rho_\lambda(T_6, \theta) L_i = L_{r,c} \quad (A7)$$

Test Specimen Luminance

The luminance of the test specimen can now be obtained by either of two methods. Solving for $L_{r,s}$ in terms of $L_{r,c}$ by use of equations (A6) and (A7) and substituting into equation (A1) gives:

$$L_s = L - L_e - \frac{\rho_\lambda(T, \theta)}{\rho_\lambda(T_6, \theta)} L_{r,c} \quad (A8)$$

Alternatively, the values of $L_{r,s}$ and $L_{r,c}$ from equations (A6) and (A7) can be substituted into equations (A1) and (A2) and solved simultaneously to obtain

$$L_s = L - \left[1 - \frac{\rho_\lambda(T, \theta)}{\rho_\lambda(T_6, \theta)} \right] L_e - \frac{\rho_\lambda(T, \theta)}{\rho_\lambda(T_6, \theta)} L_1 \quad (A9)$$

Equation (A9) is more conveniently used than equation (A8) since its use does not require an absolute measure of the reflected luminance $L_{r,c}$. Furthermore, if the ratio of the two reflectances approaches unity, the coefficient of the L_e term may become so small that this term is negligible in comparison with the other terms. The specimen luminance L_s is then approximated as the difference between the total luminance L measured with the specimen in the test stream and the total luminance L_1 measured with a water-cooled metal specimen in the stream.

The test specimen luminance L_s , as determined by equation (A9), is now equated to the integral on the right-hand side of equation (B5); hence, use of equation (B6) gives the spectral radiance of the test specimen.

The spectral radiance and the directed spectral emittance of the specimen now permit use of equation (B7) to obtain an effective black body spectral radiance. The true specimen temperature T then follows from use of the Planck black-body radiation function, equation (B2).

APPENDIX A

The preceding discussion incorporates, implicitly, two assumptions: (1) that the testing environment, though it may be radiating strongly, is optically thin and (2) that the insertion of a specimen into the testing environment has no effect on the radiation from the test gas.

Consider the first assumption. If the test gas radiation is extremely strong, part of the energy radiated from the test specimen may be absorbed in passing through the test gas. For an optically thick gas, the energy from the test specimen may be entirely absorbed, thus making pyrometric measurements of specimen properties impossible.

For all test conditions except an optically thick testing environment, absorption of radiated specimen energy may or may not be a problem depending on what information is wanted from the pyrometric measurement. If energy lost by radiation from the specimen is the primary objective, then the methods developed with the assumption of an optically thin test environment are still valid since use of these methods will give the desired net luminance of the specimen. In fact, luminances obtained from the specimen brightness temperature would be in error since they would give the total specimen luminance not the net luminance with respect to the testing environment which is the actual measure of energy lost by radiation.

On the other hand, if the specimen surface temperature is the objective of the experiment, then a measurement must be made to determine what portion of the energy from the test specimen is absorbed in passing through the test gas. Such a measurement would necessitate constructing a water-cooled model containing a radiant source of known luminance directed at the pyrometer and an optical chopper with a fixed chopping frequency. The pyrometer detector electronics would then have to incorporate alternating-current circuits sensitive only to the chopping frequency. With such a test setup, the emission-absorption methods presented in reference 5 could be used to obtain the portion of specimen luminance lost through absorption by the test gas. The measured quantities L_S , $L_{R,S}$, and $L_{R,C}$ must then be corrected for the effects of absorption in order to obtain the true value of specimen luminance.

The second assumption is valid for a subsonic gas stream such as is effluent from the facility used in this study. For a supersonic stream, however, the luminous shock wave preceding a test specimen is not present when the specimen is not in the stream. Thus the determination of luminance from the testing environment L_e is not correct for a supersonic gas stream if it is obtained by the method discussed previously. The correct value for L_e , for this method, may be obtained by use of the same water-cooled specimen used to determine whether the test gas is optically thin. This specimen is placed in the test stream with its optical chopper operating but with the radiant source not operating. Any signal obtained would give the value of luminance reflected from the cooled specimen $L_{R,C}$. A second optical chopper is then placed in the optical path

APPENDIX A

between the pyrometer and the test gas and operated at a frequency which is different from that of the first chopper but to which the pyrometer detector electronics are also sensitive. Measurements obtained with this experimental setup give the sum $L_e + L_{r,c}$. One can then proceed as before to obtain the specimen luminance.

APPENDIX B

BASIC PYROMETER RELATIONSHIPS

The luminance L of a black body at temperature T as seen through any pyrometric instrument at wavelength λ is given by (ref. 1):

$$L = \int_0^\infty N_{\lambda,b}(T) \tau'_\lambda \tau''_\lambda \tau_{\lambda,f} V_\lambda d\lambda \quad (B1)$$

where

τ'_λ spectral transmittance of all optical components in instrument through which only energy from black-body source passes

τ''_λ spectral transmittance of all components, excepting $\tau_{\lambda,f}$, common to energy from both source and energy calibration device (pyrometer lamp)

$\tau_{\lambda,f}$ spectral transmittance of wavelength limiting filters or exit slits which are also common to all energy sources

V_λ relative spectral sensitivity of energy detector

$N_{\lambda,b}(T)$ spectral radiance, found by use of Planck black-body radiation function

$$N_{\lambda,b}(T) = C_1 \lambda^{-5} \left[\exp\left(\frac{C_2}{\lambda T}\right) - 1 \right]^{-1} \quad (B2)$$

When a match is made between the luminances of the black body and the pyrometer lamp filament,

$$\int_0^\infty N_{\lambda,b}(T) K_1(\lambda) d\lambda = \int_0^\infty N_\lambda(T_1) \tau'_\lambda \tau''_\lambda \tau_{\lambda,f} V_\lambda d\lambda \quad (B3)$$

where

$N_\lambda(T_1)$ spectral radiance of pyrometer lamp filament at temperature T_1

τ'''_λ spectral transmittance of all optical components through which only energy from pyrometer lamp filament passes

$$K_1(\lambda) = \tau'_\lambda \tau''_\lambda \tau_{\lambda,f} V_\lambda$$

APPENDIX B

A series of such luminance matches for different black-body temperatures provides the instrument calibration.

A luminance match now between a real body at temperature T_2 and the pyrometer lamp filament is expressed as

$$\int_0^\infty N_\lambda(T_2) K_1(\lambda) d\lambda = \int_0^\infty N_\lambda(T_1) K_2(\lambda) d\lambda \quad (B4)$$

where, for convenience, the function $K_2(\lambda)$ is substituted for the product $\tau_\lambda' \tau_\lambda''' \tau_{\lambda,f} V_\lambda$, and it is assumed that the optical paths for the real body and the black body are essentially the same; that is, no optical components such as lenses or mirrors are in one path and not in the other. The instrument calibration allows the substitution of equation (B3) for the pyrometer lamp filament luminance to obtain

$$\int_0^\infty N_\lambda(T_2) K_1(\lambda) d\lambda = \int_0^\infty N_{\lambda,b}(T_B) K_1(\lambda) d\lambda \quad (B5)$$

where T_B (T in eq. (B3)) is the brightness temperature of the real body. Since all other terms under the integration signs are equal on both sides of the equation, it is valid to equate the spectral radiances

$$N_\lambda(T_2) = N_{\lambda,b}(T_B) \quad (B6)$$

The true temperature T_2 is then obtained from the Planck black-body radiation function (eq. (B2)) and from

$$N_{\lambda,b}(T_B) = \epsilon_\lambda(T_2, \theta) N_{\lambda,b}(T_2) \quad (B7)$$

where

$\epsilon_\lambda(T_2, \theta)$ spectral emittance of real body at temperature T_2 as observed at an angle θ from normal to body surface

$N_{\lambda,b}(T_2)$ spectral radiance of a black body at temperature T_2

REFERENCES

1. Kostkowski, H. J.; and Lee, R. D.: Theory and Methods of Optical Pyrometry. NBS Monograph 41, U.S. Dept. Com., Mar. 1, 1962. (Reprinted with corrections Sept. 1962.)
2. Paul, Fred W.: Temperature Measurements With an Optical Pyrometer Under Adverse Conditions. Appl. Opt., vol. 3, no. 2, Feb. 1964, pp. 297-301.
3. Mechtly, E. A.: The International System of Units - Physical Constants and Conversion Factors. NASA SP-7012, 1964.
4. Brown, Ronald D.; and Fowler, Bruce: Enthalpy Calculated From Pressure and Flow-Rate Measurements in High-Temperature Subsonic Streams. NASA TN D-3013, 1965.
5. Tourin, Richard H.: Monochromatic Radiation Pyrometry of Hot Gases, Plasmas, and Detonations. Temperature - Its Measurement and Control in Science and Industry, Vol. 3, Pt. 2, Reinhold Pub. Corp., c.1962, pp. 455-487.
6. Ackerman, Sumner: A Review of Automatic Radiometric Pyrometry. Temperature - Its Measurement and Control in Science and Industry, Vol. 3, Pt. 2, Reinhold Pub. Corp., c.1962, pp. 839-847.
7. Topping, J.: Errors of Observation and Their Treatment. Reinhold Pub. Corp., 1960.
8. Dow, Marvin B.; and Swann, Robert T.: Determination of Effects of Oxidation on Performance of Charring Ablators. NASA TR R-106, 1964.
9. Plunkett, J. D.; and Kingery, W. D.: The Spectral and Integrated Emissivity of Carbon and Graphite. Proceedings of the Fourth Conference on Carbon, Pergamon Press, 1960, pp. 457-472.
10. Wilson, R. Gale: Hemispherical Spectral Emittance of Ablation Chars, Carbon, and Zirconia to 3700° K. NASA TN D-2704, 1965.
11. Freemann, Mark P.; and Katz, S.: Determination of the Radial Distribution of Brightness in a Cylindrical Luminous Medium With Self-Absorption. J. Opt. Soc. Am., Vol. 50, no. 8, Aug. 1960, pp. 826-830.

"The aeronautical and space activities of the United States shall be conducted so as to contribute . . . to the expansion of human knowledge of phenomena in the atmosphere and space. The Administration shall provide for the widest practicable and appropriate dissemination of information concerning its activities and the results thereof."

—NATIONAL AERONAUTICS AND SPACE ACT OF 1958

NASA SCIENTIFIC AND TECHNICAL PUBLICATIONS

TECHNICAL REPORTS: Scientific and technical information considered important, complete, and a lasting contribution to existing knowledge.

TECHNICAL NOTES: Information less broad in scope but nevertheless of importance as a contribution to existing knowledge.

TECHNICAL MEMORANDUMS: Information receiving limited distribution because of preliminary data, security classification, or other reasons.

CONTRACTOR REPORTS: Scientific and technical information generated under a NASA contract or grant and considered an important contribution to existing knowledge.

TECHNICAL TRANSLATIONS: Information published in a foreign language considered to merit NASA distribution in English.

SPECIAL PUBLICATIONS: Information derived from or of value to NASA activities. Publications include conference proceedings, monographs, data compilations, handbooks, sourcebooks, and special bibliographies.

TECHNOLOGY UTILIZATION PUBLICATIONS: Information on technology used by NASA that may be of particular interest in commercial and other non-aerospace applications. Publications include Tech Briefs, Technology Utilization Reports and Notes, and Technology Surveys.

Details on the availability of these publications may be obtained from:

SCIENTIFIC AND TECHNICAL INFORMATION DIVISION
NATIONAL AERONAUTICS AND SPACE ADMINISTRATION

Washington, D.C. 20546